

## Effects of superparamagnetism in MgO based magnetic tunnel junctions

Weifeng Shen,<sup>1,2,\*</sup> Benaiah D. Schrag,<sup>2</sup> Anuj Girdhar,<sup>2</sup> Matthew J. Carter,<sup>2</sup> Hai Sang,<sup>3</sup> and Gang Xiao<sup>1,3,†</sup>

<sup>1</sup>*Department of Physics, Brown University, Providence, Rhode Island 02912, USA*

<sup>2</sup>*Micro Magnetics, Inc., 421 Currant Road, Fall River, Massachusetts 02720, USA*

<sup>3</sup>*Department of Physics, National Laboratory of Solid State Microstructures, Nanjing University, Nanjing 210093, China*

(Received 26 November 2008; published 14 January 2009)

We have investigated the magnetic and transport behavior of MgO based magnetic tunnel junctions incorporating  $\text{Co}_{40}\text{Fe}_{40}\text{B}_{20}$  free layers with thicknesses in the vicinity of 15 Å. The magnetic response of the free layer changes rapidly as its thickness decreases. Linear and hysteresis-free switching is obtained when the CoFeB free layer thickness is thinner than a critical thickness of  $\sim 15$  Å. The tunneling magnetoresistance and hysteresis properties of the free layer change abruptly around the critical thickness. We have analyzed the transfer curves of junctions below the critical thickness and show that they agree well with the Langevin equation describing superparamagnetism. At even lower thicknesses, the total magnetic moment of the magnetic clusters decreases rapidly, possibly due to the reduction in the magnetic ordering temperature to below room temperature.

DOI: [10.1103/PhysRevB.79.014418](https://doi.org/10.1103/PhysRevB.79.014418)

PACS number(s): 85.70.Kh, 76.60.Es, 75.70.-i, 85.75.Dd

Magnetic tunnel junctions (MTJs) with crystalline MgO barriers have been extensively studied over the last few years. Several groups have shown that proper growth and annealing conditions lead to a tunneling magnetoresistance (TMR) ratio in excess of 200%.<sup>1,2</sup> Such a high TMR has facilitated many applications in spin-based electronics, specifically in magnetic random access memory (MRAM) cells, read heads, and high-sensitivity field sensors.<sup>3,4</sup> In various applications, MTJs need to show linear and hysteresis-free switching of the free layer, which in turn requires coherent rotation of the magnetization in the free layer. A crossed magnetization pattern, in which the quiescent magnetization of the free layer is oriented perpendicular to the magnetization of the pinned reference layer, has been used to achieve this type of coherent rotation. Typically, the crossed magnetization pattern is induced by external or internal bias fields, which are generated by specialized circuitry or patterned magnetic films, or by shape anisotropy of the free layer.<sup>5-7</sup> However, each of these techniques has associated drawbacks, such as an increase in the cost and/or complexity of the fabrication process, an increase in the device power consumption or an inability to fully integrate the MTJ devices into existing complementary metal-oxide semiconductor (CMOS) circuits.

Recently, it has been found that using ultrathin magnetic films for the MTJ free layer can also introduce a linear response.<sup>8</sup> Below a critical thickness the free layer was observed to exhibit superparamagnetic behavior at the cost of a significant loss of TMR ratio.<sup>9,10</sup> Detailed studies are still not available on the nature of the magnetic state of thin free layers. For the current investigation, we fabricated a series of MTJ samples with CoFeB free layers of variable thickness and studied their magnetic properties in details using magnetometry and transport measurements. We found that the TMR ratio and hysteresis change rapidly around a critical free layer thickness (15 Å), with a linear and hysteresis-free response seen for samples whose CoFeB thickness is thinner than this critical value. This behavior is attributed to a transition of the CoFeB free layer, from the original ferromagnetic state to a superparamagnetic state, as the thickness is reduced. Based on detailed analysis on the average magnetic moment in the superparamagnetic state, we believe that the thin free layer film breaks into magnetic clusters, which behave superparamagnetically, below the critical thickness.

MTJ multilayer films were deposited on thermally oxidized Si wafers using a custom multitarget high-vacuum magnetron sputtering system under a base pressure of  $2 \times 10^{-8}$  Torr. The MTJs had the following structure (thicknesses in angstroms):

---

substrate/Ta(50)/Ru(300)/Ta(50)/ $\text{Co}_{50}\text{Fe}_{50}$ (20)/IrMn(150)/ $\text{Co}_{50}\text{Fe}_{50}$ (20)/Ru(8)/ $\text{Co}_{40}\text{Fe}_{40}\text{B}_{20}$ (30)

---

(ferromagnetic pinned layer)/MgO(20.5)/ $\text{Co}_{40}\text{Fe}_{40}\text{B}_{20}$ ( $t$ ) (magnetic free layer)/contact layer. The thickness ( $t$ ) of the  $\text{Co}_{40}\text{Fe}_{40}\text{B}_{20}$  free layer was nominally centered around 16 Å. All layers except for MgO were deposited by dc magnetron sputtering at a constant Ar pressure of 1.5 mTorr. The MgO layer was deposited by radio frequency (rf) magnetron sput-

tering at an Ar pressure of 1.1 mTorr. During the sputtering process, the substrate was rotated at a constant speed to maximize uniformity throughout the wafer. Junctions were patterned using standard optical lithography and ion milling procedures. Each sample consists of 38 elliptical junctions in series, with each junction having lateral dimensions on the

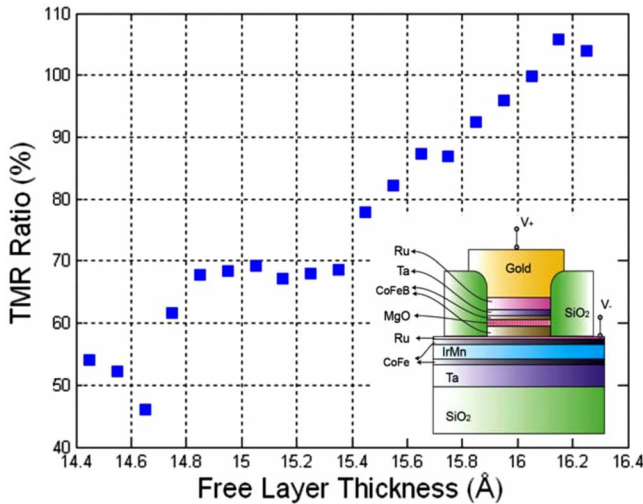


FIG. 1. (Color online) Full magnetoresistance values (TMR ratio) as a function of CoFeB free layer thickness in MgO based magnetic tunneling junctions. Inset: schematic showing the MTJ layer structure and geometry.

order of 10–150  $\mu\text{m}$ .<sup>11</sup> After patterning, the samples were annealed at 310 °C for 4 h at  $1 \times 10^{-6}$  Torr in an applied field of 6 kOe. Magnetic measurements were carried out with a vibrating sample magnetometer (VSM), while magnetotransport properties of MTJs were measured with a probe station.

All of our substrates are continuously rotated during the sputtering process, resulting in a thickness variation across each 2 in. wafer which is purely radial (with about 12% total thickness variation from center to edge). It is this smooth thickness variation that allowed us to probe the superparamagnetic behavior of the MTJ devices at room temperature. To accurately calibrate the thickness of the CoFeB free layer, we used a test structure composed of a single layer of  $\text{Co}_{40}\text{Fe}_{40}\text{B}_{20}$  sputtered on a thermally oxidized Si wafer at a constant Ar pressure of 1.5 mTorr. By patterning the film into resistive test structures with regular shapes and measuring the sheet resistance at numerous different locations, we characterized the CoFeB thickness variation across the full 2 in. wafer. The thickness data fit well to a dependence of the form  $t(r) = t_0(1 - cr^2)$ , where  $r$  is the radial position on the wafer and  $t_0$  and  $c$  were constants which were determined from fits to the data. This calibration of relative thickness is used throughout the rest of this study to determine the CoFeB thickness of hundreds of individual MTJ devices.

Figure 1 shows the measured TMR ratio as a function of the free layer thickness for representative samples across a 2 in. wafer. The TMR ratio here is defined as  $\Delta R/R_0$ , where  $R_0$  is the resistance in the parallel state (with the magnetization vectors of free and pinned layers parallel) and  $\Delta R$  is the resistance difference between the antiparallel and the parallel states. Starting at the 14.4 Å thickness, the TMR increases monotonically from about 50%–110% over a thickness change in just 2 Å. The dramatic change in TMR value over a narrow thickness range indicates that there is a significant weakening of ferromagnetic order in the free layer.

Over the same thickness range, the magnetic coercivity,

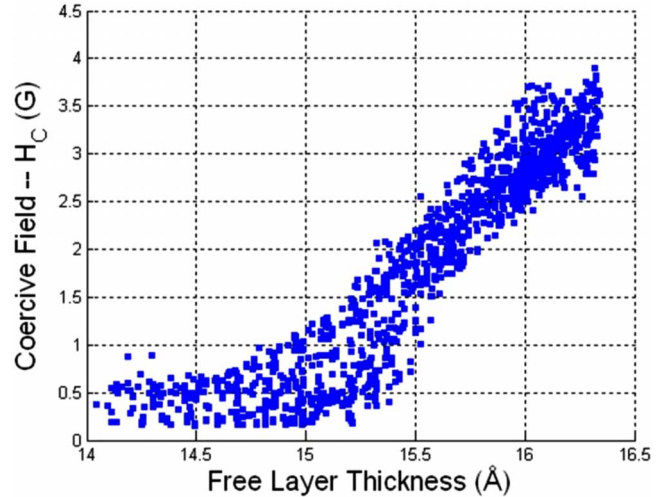


FIG. 2. (Color online) Measured magnetic hysteresis as a function of CoFeB free layer thickness for several hundred MTJ devices which were characterized.

$H_c$ , undergoes an equally dramatic change. Figure 2 shows the measured coercivity as a function of the CoFeB free layer thickness. Below what seems like a critical thickness of 15 Å, the coercivity is nearly zero. Then, starting at about 15 Å, the coercivity increases linearly with thickness. The dependence of coercivity on the thickness indicates that the free layer undergoes a magnetic transition, losing its coercive character below 15 Å. An examination of both Figs. 1 and 2 reveals that TMR value and the magnetic behavior of the free layer are strongly correlated. As the hysteresis sets in, the TMR increases correspondingly.

Figure 3 contains representative transfer curves for nine MTJ samples over a thickness range from 14.45 to 16.05 Å. Consistent with Fig. 2, transfer curves are nonhysteretic be-

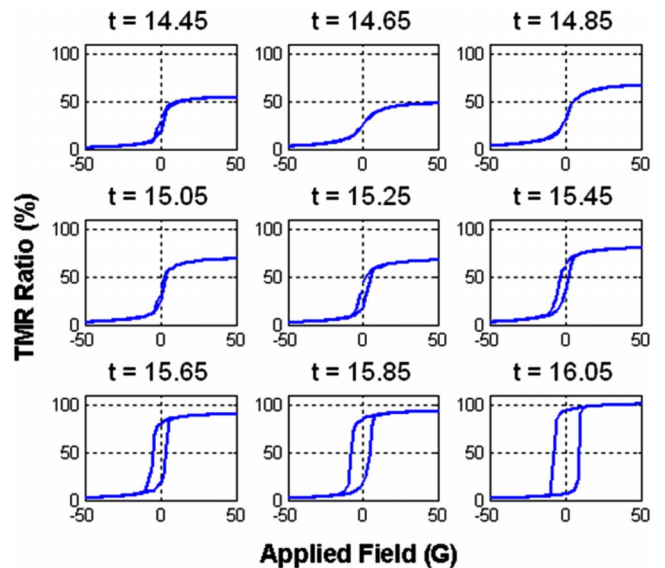


FIG. 3. (Color online) Representative transfer curves versus for a number of MTJ devices with different free layer thickness ranging from 14.45 to 16.05 Å. Note the evolution of the magnetic hysteresis.

low 15.0 Å, and gradually turn into a square shape with increasing levels of hysteresis at thicknesses above this.

The data revealed in Figs. 1–3 provide a quite unique magnetic tunneling junction system, in which the transfer curve evolves naturally from being a sensorlike response to a memorylike response over a narrow thickness range of roughly 2 Å. Engineering an MTJ sensor and a memory cell requires entirely different design and manufacturing rules. Yet, with the CoFeB free layer, one can simply use a small thickness variation to achieve these two divergent application objectives.

The weakening of ferromagnetism in thin films can be attributed to different mechanisms. As a thin film transitions from three-dimensional (3D) to two-dimensional (2D) ferromagnetism, the magnetic ordering temperature ( $T_c$ ) is often reduced. If a thin film's  $T_c$  drops below room temperature, the measured room-temperature coercivity will vanish. On the other hand, when a film is deposited thin enough, it can form magnetic islands or clusters rather than a continuous film. These magnetic clusters will be superparamagnetic as long as the ambient thermal energy is large enough to cause relaxation of the magnetization vectors of the clusters. In the superparamagnetic state, coercivity can also vanish if the measurement speed is slow relative to the relaxation rate of the magnetization.

In order to determine whether samples below 15 Å are indeed superparamagnetic, we analyzed the transfer curves using the theory of superparamagnetism. According to magnetotunneling theory, the conductance  $G$  of an MTJ is modeled as

$$G = G_0[1 + P^2 \cos(\theta_F - \theta_p)], \quad (1)$$

where  $G_0$  and  $P$  are the constants related to the resistance-area product, geometry, and overall magnetoresistance of the MTJ devices and  $\theta_F$  ( $\theta_p$ ) is the angle between the external magnetic field and the magnetization vector of the free (pinned) layer. In our measurement, because we apply the magnetic field parallel to the pinned layer magnetization (i.e.,  $\theta_p=0$ ), Eq. (1) becomes

$$\Delta G = G - G_0 \propto \cos \theta_F \propto M_F. \quad (2)$$

Therefore,  $\Delta G$  is proportional to the free layer magnetization component ( $M_F$ ) along the applied field axis.

The magnetization of an assembly of superparamagnetic clusters obeys the Langevin equation,

$$M = N\mu L\left(\frac{\mu H}{k_B T}\right), \quad (3)$$

where  $N$  is the number of magnetic clusters in a sample,  $\mu$  is the average magnetic moment of an individual cluster,  $H$  is the applied magnetic field,  $k_B$  is Boltzmann's factor,  $T$  is the temperature, and

$$L(x) = \coth(x) - \frac{1}{x}. \quad (4)$$

Figure 4(a) shows a representative MTJ transfer curve, presented in terms of  $\Delta G$ , for a sample with a free layer ( $t=14.7$  Å) thinner than the critical thickness. The solid line

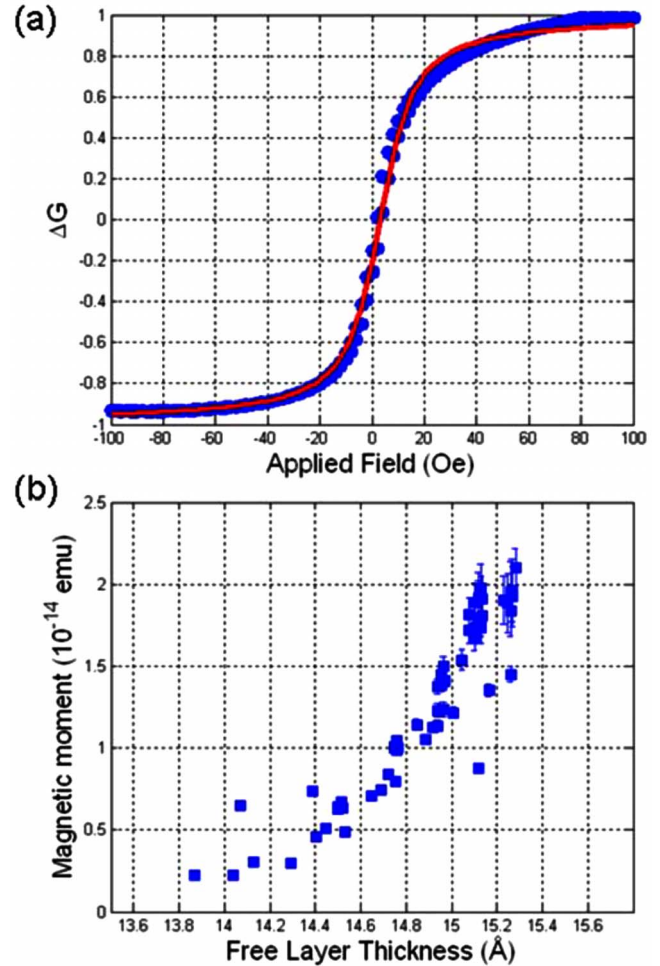


FIG. 4. (Color online) (a) A typical magnetoconductance transfer curve for an MTJ sample with a free layer thickness of 14.7 Å. The solid line represents the best fit to the data based on the Langevin equation which describes superparamagnetism. (b) Best-fit values of magnetic moment ( $\mu$ ) for several dozen samples with varying free layer thickness plotted versus free layer thickness.

represents the best theoretical fit to the data based on the Langevin equation [Eq. (3)], with  $N$  and  $\mu$  used as fitting parameters. For all curves below a certain thickness ( $t \sim 15.2$  Å), the Langevin equation predicts their magnetic behavior well, with goodness-of-fit value  $R^2 > 0.995$  for most samples.

Figure 4(b) contains the best-fit values of magnetic moment  $\mu$  for several dozen samples as a function of thickness. These samples all have best-fit  $\mu$  values on the order of  $10^{-14}$  emu (or  $10^6 \mu_B$ ), and it is clear that the average magnetic moment of the clusters and the free layer thickness are highly correlated. It is interesting to note that the fitted values of  $\mu$  decline very rapidly with thickness, dropping by an order of magnitude between  $t=15.2$  and 14.0 Å. At below 13.6 Å, the magnetic moment seems to approach zero.

Based on the range of fitted values of  $\mu$  of  $(2-20) \times 10^{-15}$  emu and using a previously reported value for the saturation magnetization  $M_S$  (860 emu/cc) of CoFeB,<sup>12</sup> we can estimate the range of volumes for the superparamagnetic particles as  $(2.4-24) \times 10^{-18}$  cm<sup>3</sup>. Assuming that our given

CoFeB thicknesses are indeed the correct values, this translates to effective lateral dimensions for the superparamagnetic particles of 40–120 nm. Relative to the thickness ( $\sim 1.5$  nm), these lateral dimensions imply that the clusters have the shape of a pancake.

Previous studies on CoFeB have shown the presence of a superparamagnetic layer, albeit generally with a smaller thickness (ranging from 3 to 8.5 Å, depending on the adjacent layers).<sup>13,14</sup> Our study suggests a more complicated scenario. As we increase the thickness of CoFeB, sputter deposition yields the formation of discrete clusters of CoFeB rather than a continuous film. These clusters are pancakelike with significantly larger lateral dimensions than thickness. Below 13.6 Å, the clusters may have magnetic ordering temperature ( $T_c$ ) less than room temperature<sup>15</sup> because the average magnetic moment of the clusters appears to extrapolate to zero around this thickness, as shown in Fig. 4(b). Measurements of these properties as a function of temperature would allow confirmation of this theory. Between 13.6 and 15.0 Å, the clusters behave superparamagnetically and the magnetic moment increases with thickness; in this thickness range, added CoFeB material likely adds to the size of existing clusters rather than forming new ones.<sup>16</sup> Above 15.0 Å they become ferromagnetic with well-defined anisotropy axes. The formation of islands of magnetic material has led to similar results in a number of other thin film systems.<sup>17–19</sup>

The monotonic reduction in the TMR value as thickness is lowered seems to be associated with the weakening of ferromagnetism. In the superparamagnetic state, the magnetization vectors can still be aligned by an external field, and the

magnetotunneling behavior remains unchanged because the electron tunneling time is much smaller than magnetization relaxation time.

In summary, we have investigated the behavior of CoFeB thin films below a critical thickness and have observed a superparamagnetic transition. Coercivity and TMR data are both strongly thickness dependent in the neighborhood of the transition and both show marked changes below this threshold. Magnetoconductance curves for all MTJ samples are well described by the Langevin equation confirming the superparamagnetic behavior. Individual superparamagnetic clusters in these CoFeB thin films have an average magnetic moment  $\mu$  on the order of  $10^{-14}$  emu, with a rapid decrease in  $\mu$  seen as the free layer thickness is decreased below the transition. Further reduction in thickness to below 13.6 Å causes the superparamagnetic moment to vanish. We attribute this behavior to a reduction in the magnetic ordering temperature which occurs inside discrete pancake-shaped clusters of CoFeB.

At Brown, the work was supported by the National Science Foundation (NSF) under Grant No. DMR-0605966 and by JHU MRSEC (NSF under Grant No. DMR-0520491). At Micro Magnetics, we were supported by National Science Foundation under Grant No. DMR-0611054. At Nanjing, support was obtained from the National Natural Science Foundation of China (NNSFC) under Grants No. 10574065 and No. 10128409 and the Chang Jiang Lecture Professorship. The authors wish to thank X. J. Zou, W. Z. Zhang, W. W. Lin, and Y. Song for discussion and assistance.

\*shen@micromagnetics.com

†gang\_xiao@brown.edu

<sup>1</sup>S. S. P. Parkin, C. Kaiser, A. Panchula, P. M. Rice, B. Hughes, M. Samant, and S. H. Yang, *Nature Mater.* **3**, 862 (2004).

<sup>2</sup>S. Yuasa, T. Nagahama, A. Fukushima, Y. Suzuki, and K. Ando, *Nature Mater.* **3**, 868 (2004).

<sup>3</sup>J. S. Moodera, L. R. Kinder, T. M. Wong, and R. Meservey, *Phys. Rev. Lett.* **74**, 3273 (1995).

<sup>4</sup>T. Miyazaki and N. Tezuka, *J. Magn. Magn. Mater.* **139**, L231 (1995).

<sup>5</sup>Y. Lu, R. A. Altman, A. Marley, S. A. Rishton, P. L. Trouilloud, G. Xiao, W. J. Gallagher, and S. S. P. Parkin, *Appl. Phys. Lett.* **70**, 2610 (1997).

<sup>6</sup>D. Lacour, H. Jaffres, F. N. Van Dau, F. Petroff, A. Vaures, and J. Humbert, *J. Appl. Phys.* **91**, 4655 (2002).

<sup>7</sup>D. Mazumdar, W. F. Shen, X. Y. Liu, B. D. Schrag, M. Carter, and G. Xiao, *J. Appl. Phys.* **103**, 113911 (2008).

<sup>8</sup>Y. Jang, C. Nam, J. Y. Kim, B. K. Cho, Y. J. Cho, and T. W. Kim, *Appl. Phys. Lett.* **89**, 163119 (2006).

<sup>9</sup>P. Wisniewski, J. M. Almeida, S. Cardoso, N. P. Barradas, and P. P. Freitas, *J. Appl. Phys.* **103**, 07A910 (2008).

<sup>10</sup>J. M. Almeida, P. Wisniewski, and P. P. Freitas, *J. Appl. Phys.*

**103**, 07E922 (2008).

<sup>11</sup>W. F. Shen, D. Mazumdar, X. J. Zou, X. Y. Liu, B. D. Schrag, and G. Xiao, *Appl. Phys. Lett.* **88**, 182508 (2006).

<sup>12</sup>S. Cardoso, C. Cavaco, R. Ferreira, L. Pereira, M. Rickart, P. P. Freitas, N. Franco, J. Gouveia, and N. P. Barradas, *J. Appl. Phys.* **97**, 10C916 (2005).

<sup>13</sup>Y. H. Wang, W. C. Chen, S. Y. Yang, K. H. Shen, C. Park, M. J. Kao, and M. J. Tsai, *J. Appl. Phys.* **99**, 08M307 (2006).

<sup>14</sup>T. Takenaga, T. Kuroiwa, J. Tsuchimoto, R. Matsuda, S. Ueno, H. Takada, Y. Abe, and Y. Tokuda, *IEEE Trans. Magn.* **43**, 2352 (2007).

<sup>15</sup>F. Huang, M. T. Kief, G. J. Mankey, and R. F. Willis, *Phys. Rev. B* **49**, 3962 (1994).

<sup>16</sup>B. Voigtlander, G. Meyer, and N. M. Amer, *Phys. Rev. B* **44**, 10354 (1991).

<sup>17</sup>J. Xu, M. A. Howson, B. J. Hickey, D. Greig, E. Kolb, P. Veillet, and N. Wiser, *Phys. Rev. B* **55**, 416 (1997).

<sup>18</sup>P. Vavassori, F. Spizzo, E. Angeli, D. Bisero, and F. Ronconi, *J. Magn. Magn. Mater.* **262**, 120 (2003).

<sup>19</sup>X. T. Tang, G. C. Wang, and M. Shima, *J. Appl. Phys.* **99**, 123910 (2006).